High temperature solution-nitriding and low-temperature nitriding of AISI 316: Effect on pitting potential and crevice corrosion performance

Bottoli, Federico; Jellesen, Morten Stendahl; Christiansen, Thomas Lundin; Winther, Grethe; Somers, Marcel A. J.

Published in:
Applied Surface Science

Link to article, DOI:
10.1016/j.apsusc.2017.06.094

Publication date:
2018

Document Version
Peer reviewed version

Elsevier Editorial System(tm) for Applied Surface Science

Manuscript Draft

Manuscript Number: APSUSC-D-17-00488R1

Title: High temperature solution-nitriding and low-temperature nitriding of AISI 316; effect on pitting potential and crevice corrosion performance

Article Type: SI: 5th Asian Conf. on HT&SE

Keywords: High nitrogen steel; low-temperature nitriding; expanded austenite; high-temperature solution nitriding; corrosion; pitting; crevice corrosion

Corresponding Author: Professor Marcel A. J. Somers, Dr. Ir.

Corresponding Author's Institution: Technical University of Denmark

First Author: Federico Bottoli, PhD

Order of Authors: Federico Bottoli, PhD; Morten S Jellesen, PhD; Thomas L Christiansen, PhD; Grethe Winther; Marcel A. J. Somers, Dr. Ir.

Abstract: Stainless steels grade AISI 316 was subjected to high temperature solution nitriding and low-temperature nitriding in order to dissolve various amounts of nitrogen in the bulk (up to approx. 0.45 wt%) and in a surface layer (up to approx. 13 wt%), respectively. Potentiodynamic polarization tests in a 0.1 M NaCl solution and crevice corrosion immersion tests in 3 wt% FeCl3 solution were studied before and after the bulk and surface treatments.
Nitrogen addition in the bulk proved to have a beneficial effect on the pitting resistance of the alloy. The formation of a zone of expanded austenite at the material surface through low-temperature nitriding resulted in a considerable improvement of the pitting potential and the crevice corrosion performance of the steels.

*Cover Letter

Dear Editor

Find attached our manuscript ” High temperature solution-nitriding and low-temperature nitriding of AISI 316; effect on pitting potential and crevice corrosion performance” to be considered for publication in the special issue of Applied Surface Science in relation to the 5th Asian Conference on Heat Treatment & Surface Engineering. The manuscript is the result of original scientific work and has not been published previously. All authors have been involved in the scientific work and have given their consent to submit this manuscript.

Looking forward to your favourable opinion.

Best regards

Marcel A.J. Somers
Head of Section, Professor

Technical University of Denmark
Department of Mechanical Engineering
Section of Materials and Surface Engineering
Produktionstorvet
Building 425, room 1.20
2800 Kgs. Lyngby
Direct phone +45 45252250
Cell phone +45 61345429

***Highlights (for review)**

Highlights:

1. High-nitrogen stainless steels were characterized with potentiodynamic electrochemistry.

2. Pitting corrosion of stainless steel is effectively mitigated by dissolving nitrogen.

3. Low temperature nitrided stainless steel has superior resistance against localized corrosion.

Graphical Abstract (for review)

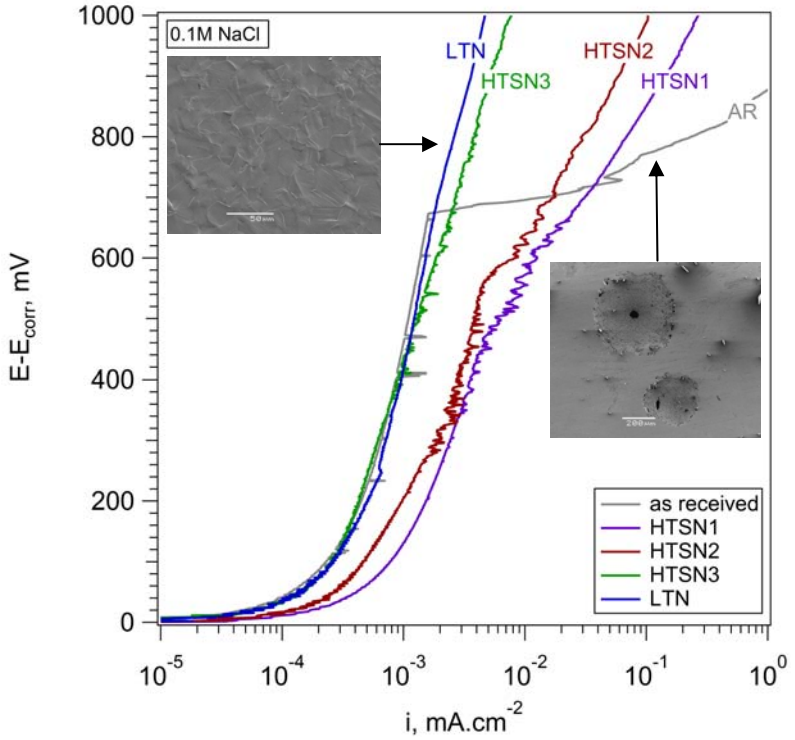

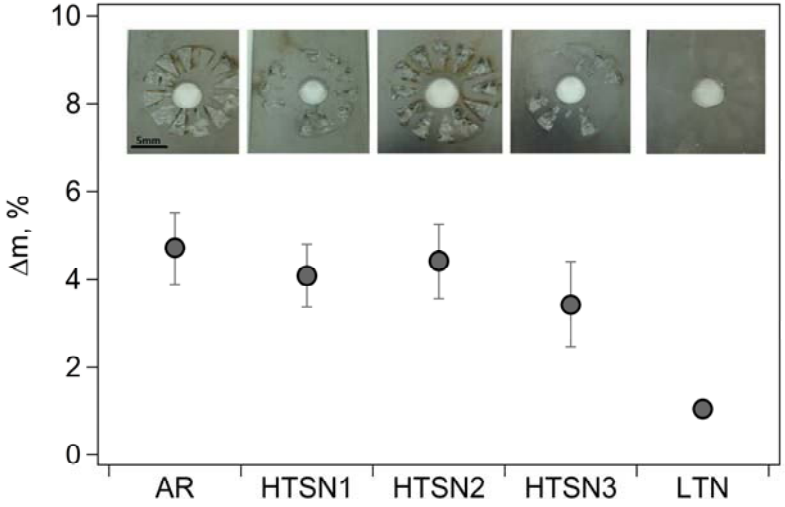

***Response to Reviewers**

Reviewers' comments:

Reviewer #1 comment	Reply- action taken
Very good work and it was a very interesting read. The following are my comments in order to improve the manuscript.	We are very pleased with the favourable opinion of the reviewer and most grateful for the comments pointed out below, which guided us in improving the manuscript. We have formulated below how we have dealt with the comments. Text changes in the manuscript have been indicated.
1) In the Introduction you mention some mechanisms which try and explain why nitrogen in solid solution increases pitting corrosion resistance. The theory of the NO3- species has been disproved because the same happens when carbon is in solid solution. In your introduction you should mention this. The works by Martin et al. should also be mentioned in the introduction because they are valid.	This has now been incorporated later in the Introduction. Since our work deals with the role of nitrogen we did not include references to carburized stainless steel in the part where we only address the behaviour of high-nitrogen steels. In the revised version we have included the literature references suggested by the reviewer to refute the explanations which are not transferable from high-nitrogen steels to the carburized case, because they entirely rely on the presence of nitrogen only. Further we have added references that have experimentally demonstrated that nitrogen leads to thinner passive layers during oxidation, which appears to be the mean reason for improved pitting resistance.
2) The text has a very good number of references however these papers are considered as important and in direct line with your work: - Buhagiar, J., Spiteri, A., Sacco, M., Sinagra, E. & Dong, H. 2012, "Augmentation of crevice corrosion resistance of medical grade 316LVM stainless steel by plasma carburising", Corrosion Science, vol. 59, pp. 169-178. - F.J. Martin, E.J. Lemieux, T.M. Newbauer, R.A. Bayles, P.M. Natishan, H.K.G.M. Michal, F. Ernst, A.H. Heuer, Carburisation induced passivity of 316L austenitic stainless steel, Electrochem. Solid State Lett. 10 (2007) C76-C78. - A.H. Heuer, H. Kahn, F. Ernst, G.M. Michal, D.B. Hovis, R.J. Rayne, F.J. Martin, P.M. Natishan, Enhanced corrosion resistance of interstitially hardened stainless steel: implications of a critical passive layer thickness for breakdown, Acta Mater. 60	These references have been included in the revised version and referred to in accordance with the reply to comment 1).

(2012) 716-725. - A.H. Heuer, H. Kahn, P.M. Natishan, F.J. Martin, L.E. Cross, Electrostrictive stresses and breakdown of thin passive films on stainless steel, Electrochim. Acta 58 (2011) 157-160. - F.J. Martin, P.M. Natishan, E.J. Lemieux, T.M. Newbauer, R.J. Rayne, R.A. Bayles, H. Kahn, G.M. Michal, F. Ernst, A.H. Heuer, Enhanced corrosion resistance of stainless steel carburized at low temperature, Metall. Mater. Trans. 40A (2009) 1805-1810. These papers should be included in your introduction and discussion of your revised text.	
3) In your introduction you use the term, "erroneously referred as S-phase". What do you mean? This is an accepted term. Please expand on this in your introduction.	We removed “erroneously”. The intention was to make clear that this is not a new phase, as suggested by the designation S-phase, but rather a supersaturated solid solution of interstitials in the f.c.c. lattice.
4) Why was 1 mV/s selected? This is a high scan rate to conduct PD tests. Please provide rationale behind this choice in the manuscript text.	Considering multiple samples and repetitions, the scan rate of 1mV/s was chosen in order to optimize testing time. We have mentioned this in the revised version.
5) In the experimental section about crevice you mention that a hole was drilled in 1 mm thick specimens. However the HTSN specimens are only 0.7 mm thick. Please fix the error or explain.	Thanks. This bug is fixed in the revised version.
6) In the crevice corrosion experiment did you control the torque used to tighten the bolt. This is very important if you want repeated results. This was not mentioned in the text and needs to be mentioned.	We did not measure the torque, but in all cases the bolt was fixed hand-tight by the same person. This is now explicitly mentioned in the revised version.
7) The amount (with a value) of the number of repeats need to be mentioned in the experimental section. Especially for the PD test and the crevice corrosion test.	In the experimental it is mentioned that the PD tests were measured at least 6 times and the crevice corrosion test twice. From the formulation by the reviewer it is unclear what additional information is requested.
8) In the captions of tables and figures you need to mention how the error +/- or error bar was calculated. You need to give the n and also the statistical method used.	This has been done in the revised version as far as this is appropriate.
9) In page 8: Why is "pore free" mentioned? This is not a coating.	We removed “pore-free” in the revised version.

10) In Figure 4: Which samples suffered crevice corrosion under the o-ring pressure? All? This needs to be mentioned in the text.	Crevice corrosion under the O-ring was observed to some extent for the HTSN treated samples, to an important extent for the annealed sample and not at all for the LTN sample. This is now mentioned in the revised version.
11) I page 11: You mentioned "statistics" but in the manuscript there is no mention of the statistics used in this work. As it was listed above, this needs to be mentioned.	What is written on p. 11 referred to improvement of the statistics by repeating the measurements more times than the two times we did this. See also comment to 7).
12) In Figure 8: A hole was drilled in the specimen. Was this hole drilled before or after the treatment? In the case of the HTSN this does not make a difference. However in the case of the LTN sample it does. Please be clear about this.	The hole was drilled after the HTSN treatments, but prior to the LTN treatment. This is now stated in the revised version.
13) Page 13: This Figure is not showing what you are saying. Double check.	On p.13 two figures are mentioned. Double checking gave the same results. We slightly rephrased the text to avoid confusion.
14) Page 13: Here you need to be very clear in which samples was crevice corrosion attack was seen.	Crevice corrosion was observed for the annealed and HTSN treated samples.
15) The highlights should not be longer than 85 characters. All your highlights are 100 characters plus. Refer to guidelines to authors.	This has been changed. We shortened the highlights to the absolute minimum, without losing significance.
16) Highlight two is not giving the exact outcome due to the fact that the crevice corrosion test was inconclusive and PD test had crevice corrosion. Please fix.	We reformulated all highlights. Now highlight two only refers to pitting corrosion, which solves the discrepancy pointed out by the reviewer.
17) The 1 week test in Ferric Chloride is very good. However you would have obtained more information if you read the OCP during the test. In that way you would have found out at what time does your crevice attack starts. The test duration might be very long. If acidified ferric chloride was used the standard dictates that the test should be 72hrs. This is a fraction of your total time.	Thanks for this additional comment. We have mentioned in the text that the testing time was 4 days longer than the recommended test duration. This could also explain why such severe attack was observed, as mentioned in the revised manuscript.

High temperature solution-nitriding and low-temperature nitriding of AISI 316; effect on pitting potential and crevice corrosion performance

Federico Bottoli, Morten S. Jellesen, Thomas L. Christiansen, Grethe Winther,

Marcel A.J. Somers

Technical University of Denmark, Department of Mechanical Engineering, Produktionstorvet

b.425, 2800 Kgs. Lyngby, Denmark

E-mail: f.bottoli@gmail.com, msj@mek.dtu.dk, tch@mek.dtu.dk, grwi@mek.dtu.dk,

somers@mek.dtu.dk

Phone: +45 45252250

Corresponding Author: Marcel A.J. Somers

somers@mek.dtu.dk

Phone: +45 45252250

Abstract

Stainless steels grade AISI 316 was subjected to high temperature solution nitriding and low-temperature nitriding in order to dissolve various amounts of nitrogen in the bulk (up to approx. 0.45 wt%) and in a surface layer (up to approx. 13 wt%), respectively. Potentiodynamic polarization tests in a 0.1 M NaCl solution and crevice corrosion immersion tests in 3 wt% $FeCl_3$ solution were studied before and after the bulk and surface treatments.

Nitrogen addition in the bulk proved to have a beneficial effect on the pitting resistance of the alloy. The formation of a zone of expanded austenite at the material surface through low-temperature nitriding resulted in a considerable improvement of the pitting potential and the crevice corrosion performance of the steels.

Keywords

High nitrogen steel, low-temperature nitriding, expanded austenite high-temperature solution nitriding, corrosion, pitting, crevice corrosion.

1 Introduction

Austenitic stainless steels are well known for their excellent corrosion resistance due to the formation of a dense chromium oxide layer at the surface. This passive film however, is susceptible to local breakdown, especially in chloride containing solutions, thereby causing localized corrosion such as pitting and crevice corrosion [1].

Stainless steels' resistance against localized corrosion can be augmented by the addition of elements such as Cr, Mo and in particular N [1]. For this reason, high nitrogen steels (HNS) have been considered as a substitute for conventional stainless steels for applications where high corrosion resistance is required [2]. Alloying with nitrogen in fact offers several advantages compared to other alloying elements in terms of corrosion and mechanical properties. Nitrogen provides a stabilization of austenite, thereby reducing the amount of expensive nickel required for minimizing the risk of forming (delta) ferrite and/or martensite upon solidification or strain-induced martensite on deformation [3]. Furthermore, nitrogen provides an important increase in yield and tensile strength, without sacrificing toughness [4–7].

The dissolution of nitrogen in austenitic stainless steels leads to a significant improvement of the crevice and pitting corrosion in aqueous solutions containing chloride ions [8–10]. Several hypotheses have been put forward to explain this behavior: (1) the presence of a high concentration of nitrogen at the steel/passive film surface stabilizing the passive film and suppressing dissolution [11–15]; (2) formation of NH_4^+ ions at the film/solution interface, neutralizing the acidity in the pit and thus promoting repassivation [16,17]; (3) formation of NO_3^- (nitrate) ions would result in improved pitting resistance [18]; (4) the austenite-stabilizing effect of nitrogen [3,4].

Despite the obvious advantages, a major obstacle to large scale application of high nitrogen stainless steels is related to their production. The solubility of nitrogen in liquid stainless steel is

limited at atmospheric pressure [19]. Hence, HNS production requires high-pressure melting technologies or the utilization of powder metallurgical production techniques [3,4,20].

On the other side, the solubility of nitrogen in the solid state is appreciably higher than in the liquid state [21]. Accordingly, post-solidification gas treatment, such as solution nitriding followed by rapid (gas) quenching [22,23] can be used to dissolve a controlled amount of nitrogen in existing steel grades. This process can be used on austenitic stainless steel grades, in order to increase the austenite stability and prevent strain-induced martensite formation [24], but also on duplex and ferritic stainless steels in order to transform ferrite and/or stabilize the austenite phase in the nitrogen enriched region [25,26].

Low-temperature surface treatment, such as low-temperature nitriding can be used to improve the surface properties of the material. This thermochemical treatment allows the dissolution of a very high amount of N (up to 38 at%) into the materials surface, and leads to the formation of a supersaturated solid solution referred to as expanded austenite [27] (~~erroneously~~ also referred to as S-Phase [28,29]). The formation of an expanded austenite case during the low-temperature nitriding (LTN) at a temperature where the precipitation of CrN from supersaturated solid solution is avoided, results in a significant improvement of the resistance to galling and, provided that no strain-induced martensite is present, improves the pitting corrosion resistance as well as the wear and fatigue resistance of the component [30–36]. A similar hardened case of supersaturated solid solutions of interstitials in austenite can also be obtained with dissolving carbon instead fo nitrogen (see for example [36]). It was demonstrated that carburized stainless steels also show significantly improved resistance against pitting and crevice corrosion [37-39]. Obviously, the improved local corrosion behavior cannot be explained from a mechanism that only considers nitrogen species as the abovementioned mechanisms 1, 2 and 3. Heuer, et al. [40,41] suggested a chemomechanical model for passive film breakdown, which essentially considers the existence of a critical thickness

of the passive film. X-ray photoelectron spectroscopical (XPS) investigations of the passive film on carburized stainless steels have shown consistently that the passive layer is thinner than on stainless steel under the same anodic polarization conditions [40,41]. An actual explanation for the thinner passive film was however not given. In this respect the detailed XPS and ellipsometry investigations of the initial oxidation of iron and iron-nitrides by Graat, et al. [42,43] demonstrated that the growth kinetics of the developing oxide layer (of the same thickness as the passive layer on stainless steel, i.e. up to 2 nm) is retarded importantly by the presence of nitrogen. This was attributed to the negative charge transfer to nitrogen atoms and the associated reduction of the electrostatic field strength over the thickness of the oxide film, which slows down the transport of cations through the film and, thus, the growth rate [42,43].

In the present work, high-temperature solution nitriding (HTSN) and low-temperature nitriding (LTN) are applied to stainless steel grade AISI 316 in order to dissolve nitrogen in the bulk and the surface, respectively. The nitriding response was studied with light-optical microscopy and X-ray diffraction. The pitting and crevice corrosion performance after the nitriding treatments was investigated with potentiodynamic measurements, immersion tests and scanning electron microscopy (SEM).

2 Experimental

2.1 Materials

The composition of the AISI 316 stainless steel used in this study is reported in Table I. The steel samples were annealed at 1323K (1050 °C) for 300s in a horizontal tube furnace with a protective high-purity argon atmosphere. Subsequently, the samples were subjected to four different treatments: three high temperature solution nitriding treatments (HTSN) and one low-temperature nitriding surface treatment (LTN).

2.1.1 High Temperature Solution Nitriding (HTSN)

High temperature gas solution nitriding is a commercial process provided by Expanite A/S [~~37~~44,~~38~~45]. Three different N_2 partial pressures were applied at 1423K (1150°C) for 4h: 0.3 bar for HTSN1, 0.6 bar for HTSN2 and 0.9 bar HTSN3. The thickness of the specimens was 0.70 mm. The duration of the treatments resulted in full homogenization and a uniform nitrogen concentration throughout the sample, indicating equilibrium between gas atmosphere and solid state. High pressure gas quench was applied to avoid formation of nitride precipitates during cooling. The nitrogen contents in the samples after treatment, as adjusted by the various applied nitrogen partial pressures, were measured with a LECO TN500 nitrogen analyzer are given in Table II. The equilibrium concentration of nitrogen that can be dissolved in the various stainless steel matrix depends on the chemical composition of the alloy [4]. Our previous work has demonstrated that the nitrogen content in the alloys can be predicted accurately by ThermoCalc, assuming equilibrium between nitrogen in the gas phase and nitrogen in austenite during HTSN [24].

2.1.2 Low-temperature nitriding (LTN)

Samples with dimensions 5x2cm^2 were obtained from the annealed steel grades. Their surfaces were ground, polished until 3µm finish and subsequently electro-polished in a “Struers Polectrol” apparatus using a “Struers electrolyte A2” with an applied potential of 30V and a current density of 2A/cm^2 to remove any deformation induced by grinding before low temperature nitriding. Low-temperature nitriding was carried out in a LAC annealing furnace model PKRC 55/09 retrofitted for gaseous nitriding under gas circulation. The sample surface was activated in-situ in order to enable the low-temperature surface hardening. The LTN process was performed at 703K (430 °C) for 20h.

2.2 Electrochemical measurements

Potentiodynamic polarization measurements were performed at room temperature using an ACM potentiostat (GillAC). The surface of the annealed and HTSN treated materials was ground and polished before and after heat treatment, and prior to electrochemical testing. For low-temperature nitriding the surface of the steel samples was ground and polished only before treatment, while electrochemical testing was performed in the as-treated condition in order not to mechanically alter the surface after the thermochemical treatment. ~~In order t~~To investigate the HTSN sample in plate geometry a flat cell set-up is required. This flat cell set-up was made of glass and a polytetrafluoro-ethylene bottom with an acrylonitrile butadiene rubber O-ring gasket, resulting in an exposed area of 0.95 cm^2 of the working electrode (sample), was used for the measurements. An Ag/AgCl electrode and a Pt wire were employed as reference and counter electrode, respectively. The open circuit potential (OCP) was monitored for 30 min prior to conducting each polarization scan. The polarization scans were conducted in naturally aerated 0.1 M NaCl solution of pH 5.2 ± 0.3. The current was measured as a function of the applied potential, starting at -0.2 V Ag/AgCl below OCP and ending at +1 V above OCP. For each sample at least six scans were measured. As this is part of a larger investigation with many samples, a relatively high scan rate of 1mV/s was chosen. ~~Each scan was repeated at least 6 times.~~

2.3 Crevice corrosion immersion tests

The crevice corrosion performance of the materials was evaluated by immersion tests ~~according to~~ inspired by, and close to, the ASTM standard G48-11 [46~~39~~]. A hole of 6 mm was drilled in the centre of ~~1~~ 0.7 mm thick samples with dimensions 5x2cm^2. For the HTSN samples the hole was drilled after HTSN treatment; for the LTN samples the hole was drilled before the LTN treatment. Two Teflon crevice washers were applied on the two parallel flat surfaces of the sample and hand-

tightened (by the same person for all samples) with bolts; the torque for fastening was not measured. Immersion tests were carried out at room temperature for 168h (1week) in a 3 wt% $FeCl_3$ solution of pH 1; the exposure time was chosen 96 hours longer than the time recommended in standard testing. The mass reduction after immersion was measured with a precision balance (0.0001 g). The crevice corrosion immersion experiments were ~~repeated~~ carried out twice.

2.4 Microstructure and materials characterization

The microstructures of the samples after HTSN and LTN were investigated in cross-section with reflected light microscopy. The samples were ground, polished and etched for 8s with Kalling´s reagent no. 1.

Microhardness indentation measurements were performed on a Future-Tech FM700 instrument using a load of 0.05 N for the evaluation of the microhardness of the "case". The surface morphology of the samples after the potentiodynamic polarization measurements was investigated with scanning electron microscopy, using a Jeol JSM-5900 microscope at an acceleration voltage of 10 kV. Glow discharge emission spectroscopy (GD-OES) was applied for the determination of the surface composition profiles after LTN treatments. The controlled sputtering of the surface was performed with a plasma at 1000Pa and 40W using a Horiba Jobin Yvon GD profiler 2. Quantification of the concentration depth-profiles was achieved using a selection of stainless steel reference materials supplemented with a custom-made γ'-Fe_4N layer on pure iron as the nitrogen reference.

3 Results

3.1 Characterization of the HTSN samples

The microstructure of the samples after HTSN was examined by XRD and LOM. The investigation revealed a significant increase in the grain size and the bulk hardness depending of the nitrogen

content dissolved. Table II summarizes the hardness and grain size after the different HTSN treatments [24]. No significant difference in grain size was found between the three HTSN treatments. This is in agreement with the experimental conditions; the treatment time and temperature for the three HTSN treatments was in fact the same. The only parameter that was changed was the partial pressure of nitrogen gas (nitrogen activity) which determines the equilibrium content of nitrogen that can be dissolved in the stainless steel.

Fig. 1 shows an isopleth of the phase diagram for AISI 316 with increasing nitrogen content as calculated with Thermocalc. Isobars of total N_2 pressures are superimposed onto the isopleth to demonstrate the range of compositions and phase stabilities that can be obtained under equilibrium between steel and gas (see Ref. 24 for details of the calculations). An excellent agreement between the experimental values and the calculated equilibrium nitrogen contents was concluded for a range of austenitic stainless steels with different compositions [24], among these the type under investigation in this work. XRD investigation (not shown) revealed that austenite is the only phase present in the as received condition and after the HTSN treatments.

3.2 Characterization of the low-temperature nitrided samples

Low-temperature nitriding was performed on the annealed condition of AISI 316. The optical micrograph in Fig. 2 shows that a homogenous ~~pore-free~~ case of expanded austenite has formed during the low-temperature surface treatment. The thickness of the obtained case is 11µm and appears virtually unattacked by the etching agent, suggesting a better corrosion resistance than the underlying substrate. The hardness of the expanded austenite zone was measured to be (1200±50) $HV_{0.05N}$.The GD-OES profiles (Fig. 3) confirm the presence of a nitrogen enriched zone at the sample surface. The nitrogen level obtained after LTN treatment is, within experimental accuracy, similar to the values obtained in the literature.

At the case-core transition a thin carbon-enriched zone is present for AISI 316 (Fig. 2) as was verified with GD-OES (Fig. 3). This carbon accumulation results from pushing carbon originally present ahead of the advancing nitrogen front [24].

X-ray diffraction analysis confirmed the formation of expanded austenite. No evidence for the presence of CrN was found in any of the samples, thereby confirming that the selected LTN process parameters avoid precipitation of nitrides.

3.3 Electrochemical Testing

Polarization curves in 0.1M NaCl solution of AISI 316 subjected to the different treatments (annealed, HTSN and LTN) are given in Fig. 4 and presented as the applied potential subtracted the corrosion potential, $E-E_{corr}$, vs. the measured current density, i. After testing, it was observed that the annealed and, to a lesser extent, HTSN samples suffer from some crevice corrosion under the O-ring; the LTN sample did not show crevice corrosion under the O-ring. This implies that the absolute value of the current density may vary from sample to sample, because the effective exposed surface area varies. For this reason the polarization curves are only interpreted qualitatively with respect to the resistance against localized corrosion, as characterized by a sudden increase in the current density, which is independent of the absolute value of the current density.

The polarization curve for the annealed condition shows a sudden and rapid increase of the anodic current density (675 mV above E_{corr}), indicating breakdown of the passive film and pit initiation. The dissolution of (additional) nitrogen in the stainless steel matrix by HTSN results in a significant change in the corrosion behavior. After the HTSN treatments, no sudden increase is observed in the current density that could indicate a breakdown of the passive film in the potential scan region up to 1000 mV Ag/AgCl. Rather, after $E-E_{corr}$ reaches approximately 200 mV Ag/AgCl, oscillations in the anodic current are observed, which may indicate pit initiation and fast re-passivation. It is no

longer possible to identify a potential where passive film breakdown occurs, indicating that the amount of nitrogen promotes passivation of the stainless steel. For the LTN treated samples, no indications of passive film breakdown were observed. Polarization curves show fewer oscillations for the LTN treated sample than for the HTSN treated samples.

Secondary electron images confirmed the presence of large pits for the annealed condition after electrochemical testing (Fig. 5), consistent with the polarization curve AR (1) in Fig. 4.The HTSN treated samples hardly show any evidence of localized corrosion detected by visual inspection. In Fig. 6 the surface morphology of the AISI 316 samples after HTSN treatment and polarization tests is presented. Scanning electron microscopical investigation indicates the presence of small pits, which would be consistent with the hypothesis that pits do form, but that their growth is impaired by repassivation. The pit formation followed by subsequent repassivation is consistent with the oscillation in the anodic current, as recorded for these samples during the polarization measurements (Fig. 4 for HTSN samples).

The surface morphology after the potentiodynamic measurements of the LTN treated AISI 316 is shown in Fig. 7. Visual inspection did not reveal any large pits and the SEM investigation shows no indication of localized corrosion such as pitting or grain boundary corrosion. However, the surface morphology of the nitrided samples differs importantly from the as-received and the HTSN-treated samples (Fig. 7). The LTN sample has a significantly increased surface roughness as an immediate consequence of the nitriding process. The presence of slip lines in Fig. 7 is a consequence of plastic deformation accommodation (and associated lattice rotation) of composition-induced strains as generated by the volume expansion caused by dissolution of a high amount of nitrogen [40]. The increase in surface roughness implies that the “exposed” area through which the current density shown in Fig.4 is measured, is larger than the nominal (projected) area, which was used in the calculation of the polarization curves. Hence, taking surface roughness into account, the current

density for the LTN sample is actually lower than the nominal value depicted in the polarization curve (Fig. 4).

3.4 Crevice Corrosion Performance Testing in $FeCl_3$ Solution

Macroscopic images of the crevice corrosion tested samples are collected in Fig. 8. Generally, the steels in the annealed and the HTSN treated conditions show severe crevice corrosion attack. No obvious difference can be discerned between these samples, indicating that, for the severe and extended exposure conditions applied here, it is not possible to conclude whether the HTSN treatment has actually improved the crevice corrosion performance. On the other hand, the optical appearance of the LTN treated sample shows a dramatic improvement of corrosion attack in the crevices between samples and Teflon washers, in particular since the severe test was extended to 168 hours instead of 72 hours . The weight loss of the samples after the immersion tests is displayed. Consistent with the images in Fig. 8 a slightly decreasing trend is observed in the weight loss of the as-received and HTSN treated samples, but within experimental accuracy no reduction in weight loss is observed after HTSN treatment. In this respect it is mentioned that the error bars are relatively large and obscure a possible improvement by the HTSN treatment. It is expected that in order to improve the statistics more samples need to be investigated if this test has to be used to rank the treatments. In contrast, the dissolution of a “colossal” amount of nitrogen (up to 38 at% [4~~81~~–50~~43~~]) into the stainless steel surface by low-temperature nitriding has led to a significant reduction of the weight loss in the crevice corrosion performance test. This result is consistent with the corresponding images in Fig.8 and the above-mentioned interpretation of the potentiodynamic results in Fig. 4.

4 Discussion

Stainless steels derive their excellent corrosion performance from the presence of a self-healing chromium-based (oxy)hydroxide film at the material´s surface. Nevertheless, stainless steels can suffer from localized corrosion, or pitting, which may well be negligible in terms of weight loss, but often is detrimental. The resistance against localized corrosion can be improved by adding more of the substitutional alloying elements Cr and Mo. In particular the addition of interstitial nitrogen is most efficient in increasing the pitting resistance equivalent number (PREN=%Cr + 3.3(%Mo) + 16(%N)) [~~44~~51]. Compared to HTSN, LTN allows dissolution of up to 38 at% nitrogen into the material´s surface [4~~81~~–50~~43~~]. Assuming that the equation given above is valid also for very high nitrogen contents, the PREN numbers for the investigated treatments are given in Table III. Clearly, after HTSN, the PREN number increases gradually with the increasing concentration of dissolved nitrogen. On the other hand, due to the colossal amount of nitrogen at the surface after LTN, this value increases dramatically to approx. 180, since the nitrogen has a much stronger effect (factor 16 in the equation).

The present experimental results confirm improved resistance against pitting with an increase in nitrogen content, and thus the PREN number. In particular for the low-temperature nitrided material, no evidence of pitting after polarization was found after polarization in the investigated potential range. These results reflect what has also been observed in other research activities on expanded austenite [52~~45~~–5~~47~~]. The polarization curves in Fig. 4 show that the dissolution of nitrogen in AISI 316 by low-temperature nitriding leads to a more stable passive layer.

For the steel investigated, a high concentration of nitrogen at the surface, obtained through the low-temperature nitriding process, does not reveal any indication of pit formation. This is confirmed by SEM investigations (Fig.7). The behaviour of dramatically higher improved pitting resistance is comparable to alloys which contain higher alloying contents of particularly Cr and Mo. The present

results are in agreement with what has been found in previous research activities [33,37-39,5245,54,55,7,5992–5461] and are believed to be due to the high concentration of nitrogen at the interface between the passive film and the steel, which suppresses further dissolution of the metal [11–13]. The effect of nitrogen addition on the current density in the anodic region of the polarization curve was widely published in the literature; so far controversial results have been reported. Several researchers claim that it provokes a decrease of the current density, while others claim that it has no or the opposite effect [10,4956,5158–5663]. In the case examined herepresent work (Fig. 6), intercomparison of thethe investigated HTSN treated samples shows a clear relation between the current density in the anodic region and the dissolved nitrogen content (Fig. 6): the current density in the passive region is reduced to lower values the for higher the nitrogen content the lower is the current density in the passive region. HoweverNevertheless, the current densities measured on the HTSN1 and HTSN2 treated samples are still higher than for the annealed condition. This may be associated with the test set-up, which cannot prevent crevice corrosion under the O-ringIn this respect it is mentioned that the as annealed (300s at 1323 K) sample has a different thermal history than the three HTSN samples (additionally 4 h at 1423 K), which may have an influence on the crystallographic texture as well as the grain size (cf. Table II). The difference between HTSN and annealed samples was not further investigated.

Low temperature thermochemical treatment however causes a decrease of the current density as also indicated in other research activities in a wide range of solutions [4552–4754,5764].

It has been reported in literature that high nitrogen steels exhibit better crevice corrosion performance than stainless steels without nitrogen addition, as reflected by a trend towards lower weight loss and the fewer corrosion spots [4552,4855,5764]. Apparently, the nitrogen present in solid solution or in the surface-adjacent region is dissolved in the aqueous environment filling the crevice and contributes importantly to the suppression of (further) corrosion attack.

In the present investigation, the immersion tests did not reveal a significant improvement in the crevice corrosion performance after enhancing the nitrogen content in the bulk with HTSN. Such a trend is not possible to reveal in the current investigation due to the aggressiveness of the 3 wt% $FeCl_3$ solution at pH 1. On the other hand, in the LTN treated materials, a dramatically reduced corrosion attack is observed. These findings confirm the results obtained in other activities for which the weight loss is significantly reduced as a consequence of the low-temperature thermochemical treatments.

The significantly higher nitrogen content in expanded austenite is effective in mitigating crevice corrosion attack. It is important to mention that an improvement of the crevice corrosion performance by a high nitrogen content requires that nitrogen is not bound to CrN precipitates to such a degree that the Cr content in solid solution is insufficient for passivation of the surface.

From the polarization curves for annealed and LTN treated AISI 316 in Fig. 4 it follows that accelerated pitting corrosion attack of the substrate can be expected upon breakthrough of the expanded austenite case. Overlap of LTN and HTSN3 polarization curves shows that a remedy for such corrosion attack is an HTSN treatment with as high a nitrogen content as possible.

5 Conclusion

Austenitic stainless steel grade AISI 316 was subjected to high-temperature solution nitriding (HTSN) treatments or low-temperature nitriding (LTN).

The HTSN treatment allows an increase of the nitrogen content in the bulk, which contributes to an improvement of the pitting resistance (high pitting potential) of the alloy, as compared to the untreated material. No improvement was observed in the crevice corrosion performance test of HTSN treated material. Such an improvement may be obscured by the aggressiveness of ferric chloride solution used for present investigations.

The LTN process leads to the formation of a nitrogen-rich case at the material surface. The processing parameters (nitriding temperature and time) allowed the formation of a supersaturated solid solution of nitrogen without the precipitation of CrN. The nitrogen dissolved during the LTN process was significantly higher than obtained with a HTSN process and allowed a major improvement of the resistance against localized corrosion of the investigated steels.

Crevice corrosion immersion tests of the LTN material showed a dramatic reduction of the weight loss as compared to the untreated and HTSN treated materials, despite extended exposure to ~~the~~ a harsh environment.

All results indicate that nitrogen has an important effect on the localized corrosion performance.

Acknowledgement

For part of the present research work, the authors gratefully acknowledge the Research Fund for Coal and Steel for financial support to the PressPerfect project.

References

[1] L. Shreir, R.A. Jarman, G.T. Burstein, Materials and Corrosion, 3rd ed., Butterworth-Heinemann, Oxford, 1994.

[2] M.O. Speidel, Properties and applications of high nitrogen steels, in: A. Hendry, J. Foct (Eds.), Proceedings International Conference HSN 88 Lille, The insitute of Metals, London, 1989, p. 92.

[3] R. Reed, Nitrogen in austenitic stainless steels, JOM. 41 (1989) 16–21.

[4] J. Simmons, Overview: high-nitrogen alloying of stainless steels, Mater. Sci. Eng. A. 207 (1996) 159–169.

[5] E. Werner, Solid solution and grain size hardening of nitrogen-alloyed austenitic steels, Mater. Sci. Eng. 101 (1988) 93-98.

[6] L.Å. Norström, The influence of nitrogen and grain size on yield strength in Type AISI 316L austenitic stainless steel, Met. Sci. 11 (1977) 208–212.

[7] Y. Takahashi, K. Yoshida, M. Shimada, E. Tada, Mechanical evaluation of nitrogen-strengthened stainless steels at 4K, Adv. Cryog. Eng. Mater. 28 (1982) 73–81.

[8] J.R. Kearns, H.E. Deverell, Use of nitrogen to improve the corrosion resistance of FeCrNiMo alloys for the chemical process industries, Mater. Perform. 26 (1987) 18–28.

[9] M. Janik-Czachor, Effect of nitrogen content in a 18Cr-5Ni-10Mn stainless steel on the pitting susceptibility in chloride solutions, Corrosion. 31 (1975) 394 – 398.

[10] J.J. Eckenrod, C.W. Kovach, Effect of Nitrogen on the Sensitization, Corrosion and

Mechanical Properties of 18Cr-8Ni Stainless Steel, in: C.R. Brinkman, H.W. Garvin (Eds.) Properties of Austenitic Stainless Steels and Their Weld Metals, American Society for Testing and Materials (ASTM), Philadelphia, 1979, pp. 17–41.

[11] Y.C. Lu, R.. Bandy, C.R. Clayton, R.C. Newman, Surface enrichment of nitrogen during passivation of a highly resistant stainless steel, J. Electrochem. Soc. 130 (1983) 8.

[12] I. Olefjord, L. Wegrelius, Role of nitrogen on the corrosion behavior of austenitic stainless steels, Corros. Sci. 38 (1996) 1203–1220.

[13] C.O.A. Olsson, The influence of nitrogen and molybdenum on passive films formed on the austenoferritic stainless steel 2205 studied by AES and XPS, Corros. Sci. 37 (1995) 467–479.

[14] A. Scrinivasan, B. Reynders, H.J. Grabke, Localised corrosion behaviour of high and low nitrogen Cr-Mn steels, Steel Res. 66 (1995) 439–443.

[15] S. Ahila, B. Reynders, H.J. Grabke, The evaluation of the repassivation tendency of Cr-Mn and Cr-Ni steels using scratch technique, Corros. Sci. 38 (1996) 1991–2005.

[16] K. Osozawa, The Effect of Nitrogen on the Corrosion Resistance of Stainless Steels, Japan Soc. Heat Treat. 36 (1985) 206–212.

[17] K. Osozawa, N. Okato, Y. Fukase, K. Yokota, N, Boshoku Gjtutsu (Corros. Eng.). 24 (1975) 1.

[18] H.P. Leckie, H.H. Uhlig, Environmental Factors Affecting the Critical Potential for Pitting in 18–8 Stainless Steel, J. Electrochem. Soc. 113 (1966) 1262.

[19] A.H. Satir-Kolorz, H.K. Feichtinger, On the solubility of nitrogen in liquid iron and steel alloys using elevated pressure, Zeitschrift Fuer Met. Res. Adv. Tech. 82 (1991) 689–697.

[20] G. Stein, I. Hucklenbroich, Manufacturing and Applications of High Nitrogen Steels, Mater. Manuf. Process. 19 (2004) 7–17.

[21] K.F. M. Kikuchi, M. Kajihara, Solubility of nitrogen in austenitic stainless steels, in: A. Hendry, J. Foct (Eds.), Proceedings International Conference HSN 88 Lille, The insitute of Metals, London, 1989, p. 63.

[22] H. Berns, Manufacture and Application of High Nitrogen Steels, ISIJ Int. 36 (1996) 909–914.

[23] H. Berns, S. Siebert, High Nitrogen Austenitic Cases in Stainless Steels, ISIJ Int. 36 (1996) 927–931.

[24] F. Bottoli, G. Winther, T.L. Christiansen, K. V. Dahl, M.A.J. Somers, Low-temperature nitriding of deformed austenitic stainless steels with various nitrogen contents obtained by prior high temperature solution nitriding, submitted to Metallurgical and Materials Transaction A (2016) 4146-4159.

[25] C.M. Garzón, A.P. Tschiptschin, New high temperature gas nitriding cycle that enhances the wear, J. Mater. Sci. 39 (2004) 7101 – 7105.

[26] A.P. Tschiptschin, Predicting Microstructure Development During High Temperature Nitriding of Martensitic Stainless SteelsUsing Thermodynamic Modeling, Mater. Res. 5 (2002) 257–262.

[27] T.L. Christiansen, M.A.J. Somers, Low-temperature gaseous surface hardening of stainless steel: the current status, Int. J. Mater. Res. Former. Zeitschrift Fuer Met. 100 (2009) 1361–1377.

[28] H. Dong, S-phase surface engineering of Fe-Cr, Co-Cr and Ni-Cr alloys, Int. Mater. Rev. 55 (2010) 65–98.

[29] T. Bell, Current Status of Supersaturated Surface Engineered S-Phase Materials, Key Eng. Mater. 373-374 (2008) 289–295.

[30] Z. Yu, X. Xu, L. Wang, J. Qiang, Z. Hei, Structural characteristics of low-temperature plasma-nitrided layers on AISI 304 stainless steel with an ~~α9~~ α' -martensite layer, 153 (2002) 125–130.

[31] M.K. Lei, X.M. Zhu, Plasma-based low-energy ion implantation of austenitic stainless steel for improvement in wear and corrosion resistance, Surf. Coatings Technol. 193 (2005) 22–28.

[32] Y. Sun, T. Bell, Sliding wear characteristics of low temperature plasma nitrided 316 austenitic stainless steel, Wear. 218 (1998) 34–42.

[33] C.. Li, T. Bell, Corrosion properties of active screen plasma nitrided 316 austenitic stainless steel, Corros. Sci. 46 (2004) 1527–1547.

[34] Committee of Stainless Steel Producers, Review of the Wear and Galling Characteristics of Stainless Steels, American Iron and Steel Institute, Washington, 1978.

[35] M.A.J. Somers, T. Christiansen, Kinetics of Microstructure Evolution during Gaseous Thermochemical Surface Treatment, J. Phase Equilibria Diffus. 26 (2005) 520–528.

[36] T. Bell, Surface engineering of austenitic stainless steel, Surf. Eng. 18 (2002) 415–422.

[37] F.J. Martin, E.J. Lemieux, T.M. Newbauer, R.A. Bayles, P.M. Natishan, H.K.G.M. Michal, F. Ernst, A.H. Heuer, Carburisation induced passivity of 316L austenitic stainless steel, Electrochem. Solid State Lett. 10 (2007) C76-C78.

[38] F.J. Martin, P.M. Natishan, E.J. Lemieux, T.M. Newbauer, R.J. Rayne, R.A. Bayles, H. Kahn, G.M. Michal, F. Ernst, A.H. Heuer, Enhanced corrosion resistance of stainless steel carburized at low temperature, Metall. Mater. Trans. 40A (2009) 1805-1810.

[39] Buhagiar, J., Spiteri, A., Sacco, M., Sinagra, E. & Dong, H. 2012, "Augmentation of crevice corrosion resistance of medical grade 316LVM stainless steel by plasma carburising", Corrosion Science, vol. 59, pp. 169-178.

[40] A.H. Heuer, H. Kahn, P.M. Natishan, F.J. Martin, L.E. Cross, Electrostrictive stresses and breakdown of thin passive films on stainless steel, Electrochim. Acta 58 (2011) 157-160.

[41] A.H. Heuer, H. Kahn, F. Ernst, G.M. Michal, D.B. Hovis, R.J. Rayne, F.J. Martin, P.M. Natishan, Enhanced corrosion resistance of interstitially hardened stainless steel: implications of a critical passive layer thickness for breakdown, Acta Mater. 60 (2012) 716-725.

[42] P.C.J. Graat, M.A.J. Somers, E.J. Mittemeijer, The oxidation of ε-Fe_2N_{1-x}; and XPS investigation, Appl. Surf. Sci. 136 (1998) 238-259

[43] P.C.J. Graat, M.A.J. Somers, E.J. Mittemeijer, The initial oxidation of ε-Fe_2N_{1-x}; growth kinetics, Thin Solid Films, 353 (1999) 72-78.

[~~37~~44]T.L. Christiansen, T.S. Hummelshøj, M.A.J. Somers, Solution hardening of cold deformed passive alloy workpiece used to form component e.g. lock washer, involves dissolving nitrogen in workpiece and cooling in presence of inert gas which does not contain nitrogen at preset temperature, WO2013159781-A1, 2013.

[3845]T.L. Christiansen, T.S. Hummelshøj, M.A.J. Somers, Forming expanded austenite and/or expanded martensite by solution hardening of cold deformed workpiece of passive alloy, WO2012 146254-A1, 2012.

[3946]Standard test methods for pitting and crevice corrosion resistance of stainless steels and related alloys by use of ferric Chloride solution, ASTM Int. 03 (2003) 1–10.

[407] C. Templier, J.C. Stinville, P. Villechaise, P.O. Renault, G. Abrasonis, J.P. Rivière, A. Martinavičius, M. Drouet, On lattice plane rotation and crystallographic structure of the expanded austenite in plasma nitrided AISI 316L steel, Surf. Coatings Technol. 204 (2010) 2551–2558.

[4148]T.L. Christiansen, M.A.J. Somers, Low temperature gaseous nitriding and carburising of stainless steel, Surf. Interface Anal. 21 (2005) 445–455.

[4249]C. Blawert, H. Kalvelage, B.L. Mordike, G.A. Collins, K.T. Short, Y. Jirásková, et al., Nitrogen and carbon expanded austenite produced by PI3, Surf. Coatings Technol. 136 (2001) 181–187.

[4350]Z. Cheng, C.X. Li, H. Dong, T. Bell, Low temperature plasma nitrocarburising of AISI 316 austenitic stainless steel, Surf. Coatings Technol. 191 (2005) 195–200.

[4451]I. Olefjord, Surface Composition of Stainless Steels during Anodic Dissolution and Passivation Studied by ESCA, J. Electrochem. Soc. 132 (1985) 2854.

[4552]D. Formosa, R. Hunger, A. Spiteri, H. Dong, E. Sinagra, J. Buhagiar, Corrosion behaviour of carbon S-phase created on Ni-free biomedical stainless steel, Surf. Coatings Technol. 206 (2012) 3479–3487.

[4653]A. Fossati, E. Galvanetto, T. Bacci, F. Borgioli, Improvement of corrosion resistance of austenitic stainless steels by means of glow-discharge nitriding, Corros. Rev. 29 (2011) 209–221.

[4754] J. Buhagiar, H. Dong, Corrosion properties of S-phase layers formed on medical grade austenitic stainless steel, J. Mater. Sci. Mater. Med. 23 (2012) 271–281.

[4855]H. Baba, Y. Katada, Effect of nitrogen on crevice corrosion in austenitic stainless steel, Corros. Sci. 48 (2006) 2510–2524.

[4956]H. Baba, T. Kodama, Y. Katada, Role of nitrogen on the corrosion behavior of austenitic stainless steels, Corros. Sci. 44 (2002) 2393–2407.

[5057]J. Buhagiar, H. Dong, T. Bell, Low temperature plasma surface alloying of medical grade austenitic stainless steel with carbon and nitrogen, Surf. Eng. 23 (2007) 313–317.

[5158]H. Yashiro, D. Hirayasu, N. Kumagai, Effect of Nitrogen Alloying on the Pitting of Type 310 Stainless Steel, ISIJ Int. 42 (2002) 1477–1482.

[5259]H. Yashiro, D. Takahashi, N. Kumagai, K. Mabuchi, Effect of Nitrogen and Molybdenum Species on the Pitting of Stainless Steel in High-Temperature Chloride Solutions, Corros. Eng. 47 (1998) 591.

[5360]H. Ohno, H. Tanabe, A. Sakai, T. Misawa, Corros. Eng. 47 (1998) 584.

[5461]G.C. Palit, V. Kain, H.S. Gadiyar, Electrochemical Investigations of Pitting Corrosion in Nitrogen-Bearing Type 316LN Stainless Steel, Corrosion. 49 (1993) 977–991.

[5562]T. Komori, U. Nakada, Electrochemical Behavior of Nitrogen-Bearing Austenitic Stainless Steels, in: Proceedings 39th Japan Corros. Conf. JSCE, 1992: p. 353.

[5663]M. Janik-Czachor, E. Lunarska, Z. Szklarska-Smialowska, Effect of Nitrogen Content in a 18Cr-5Ni-10Mn Stainless Steel on the Pitting Susceptibility in Chloride Solutions, Corrosion. 31 (1975) 394–398.

[5764]J. Buhagiar, S-Phase for biomedical applications: an interdisciplinary approach, in: 6th Ed. Interdiscip. Eng., “Petru Maior” University of Tirgu Mures, Romania, 2012: pp. 10–16.

Figure captions

Figure 1: Isopleth in the phase diagram for AISI 316 showing the phase stability of austenite in the temperature range 1223-1623K (950-1350 °C) vs. nitrogen content in the solid state. Superimposed on the isopleth, N_2 isobars are given that would provide the corresponding equilibrium nitrogen contents.

Figure 2: Reflected light micrograph on low-temperature nitrided AISI 316, after etching with Kalling´s reagent no. 1 for 8 seconds.

Figure 3: GD-OES Compositional depth profiles for nitrogen and carbon after low-temperature nitriding.

Figure 4: Polarization curves for the AISI 316 in annealed condition (AR), after HTSN treatment and after LTN surface treatment.

Figure 5: SEM micrograph showing the pits formed in the annealed AISI 316 after the potentiodynamic measurements.

Figure 6: SEM micrographs showing the surface morphology of the AISI 316 HTSN treated samples after the potentiodynamic measurements: (a) HTSN1, (b) HTSN2, (c) HTSN3.

Figure 7: SEM micrograph of the AISI 316 LTN after the potentiodynamic measurements.

Figure 8: Weight loss after crevice corrosion immersion tests of AISI 316 after various treatments. The tests were performed in a 3 wt-% $FeCl_3$ pH≈1 solution for 168 h. The micrographs show the attack at the location of the Teflon washer. The error bars represent the highest and lowest value (of 2) measured for the mass loss.

Tables

Table I: Chemical composition AISI 316 in wt% as provided by the suppliers, Lemvigh Muller.

	C	Si	Mn	Cr	Ni	Mo	N	S
AISI 316	0.07	0.4	1.6	17.0	10.55	2.0	0.05	≤0.030

Table II: Nitrogen content, [N], grain size, <D>, and Vickers hardness, HV_{2N}, of AISI 316 after high temperature solid solution nitriding. Indicated +/- ranges refer to uncertainty in the measurement (for [N]), standard variation of grain size measurement and hardness (<D>, HV).

	[N] (wt%)	<D> (µm)	HV_{2N}
AR	0.05	14±3	170±10
HTSN1	0.306±0.001	50±8	222±9
HTSN2	0.407±0.002	50±8	231±8
HTSN3	0.448±0.002	51±7	238±10

Table III: PREN numbers calculated for the investigated HTSN and LTN treatments of AISI 316.

	AR	HTSN1	HTSN2	HTSN3	LTN
PREN	24.4	28.5	30.1	30.8	≈180

Figure 1

Click here to download high resolution image

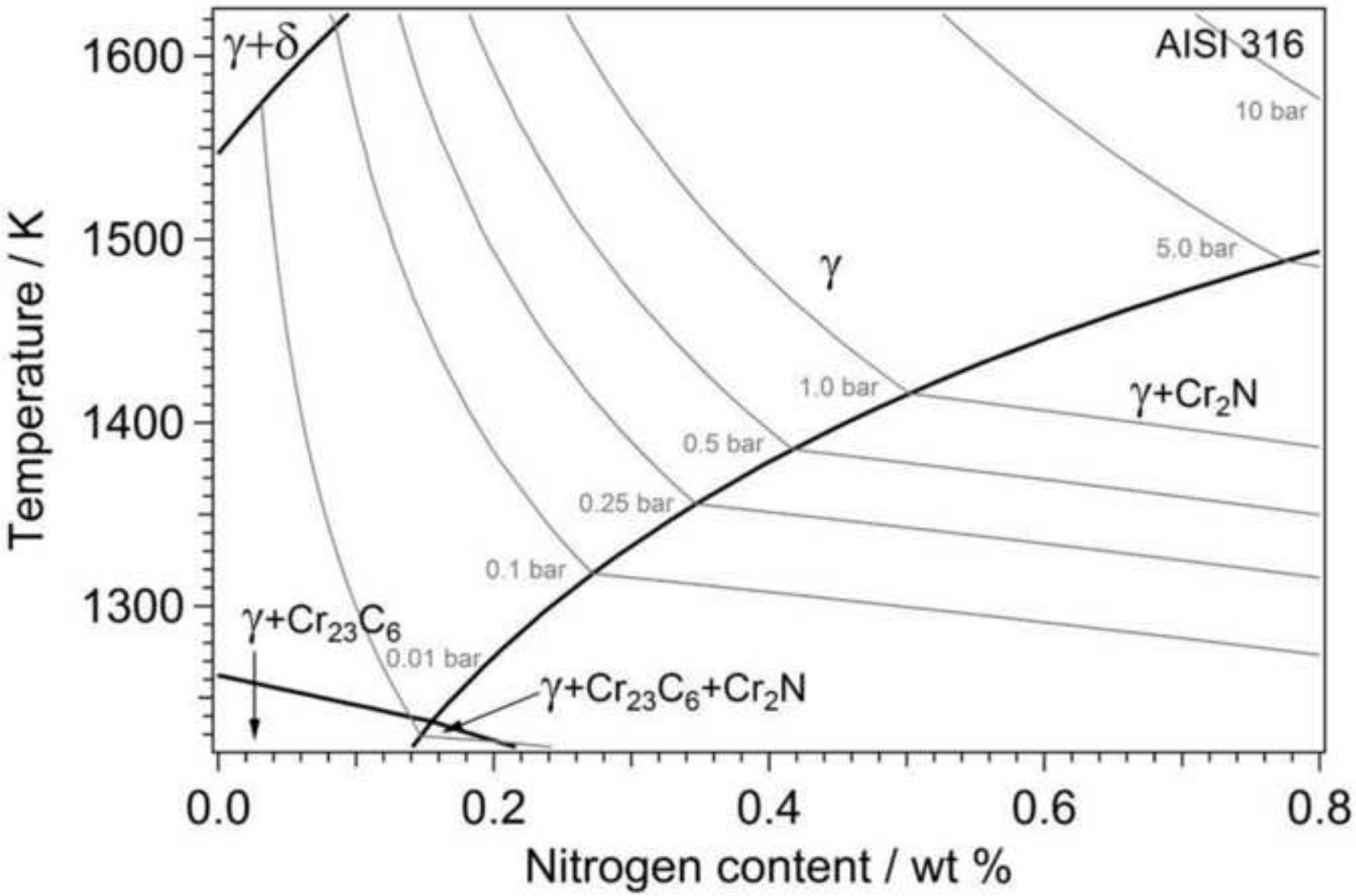

Figure 1a

Figure 2

Click here to download high resolution image

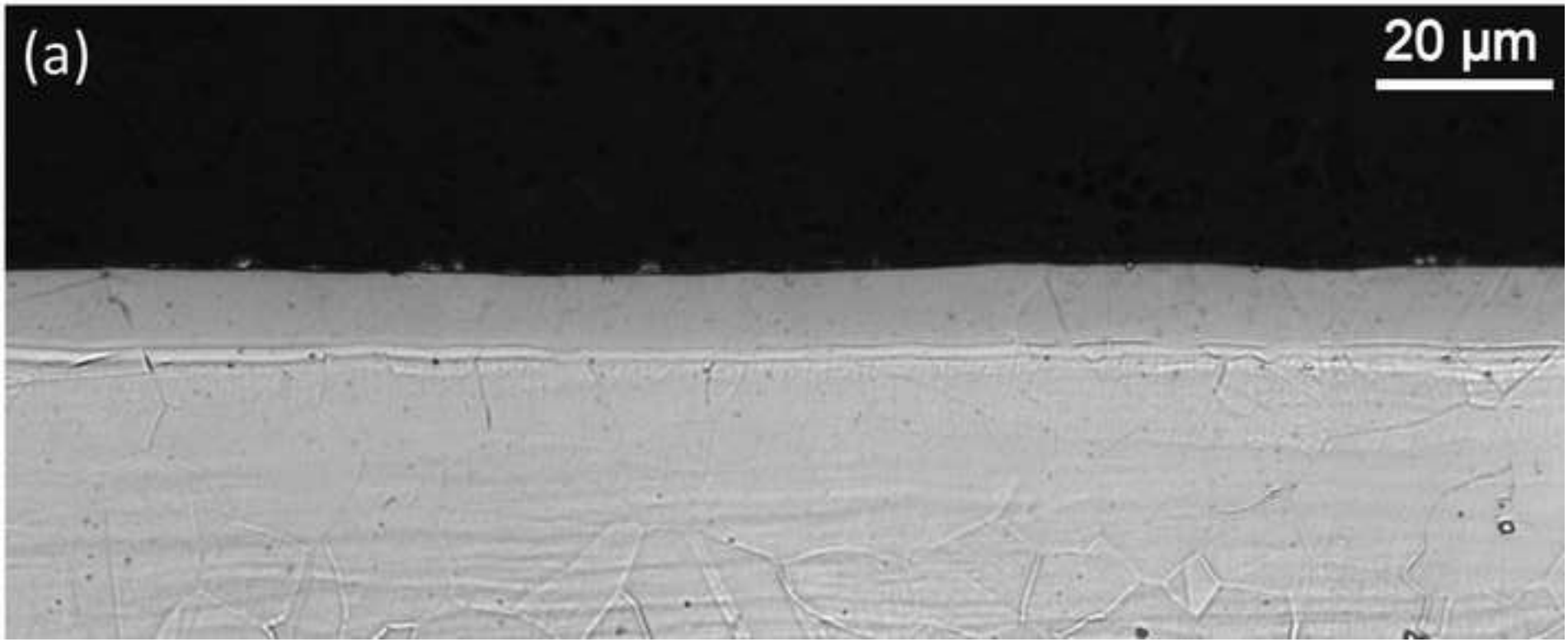

Figure 3

Click here to download high resolution image

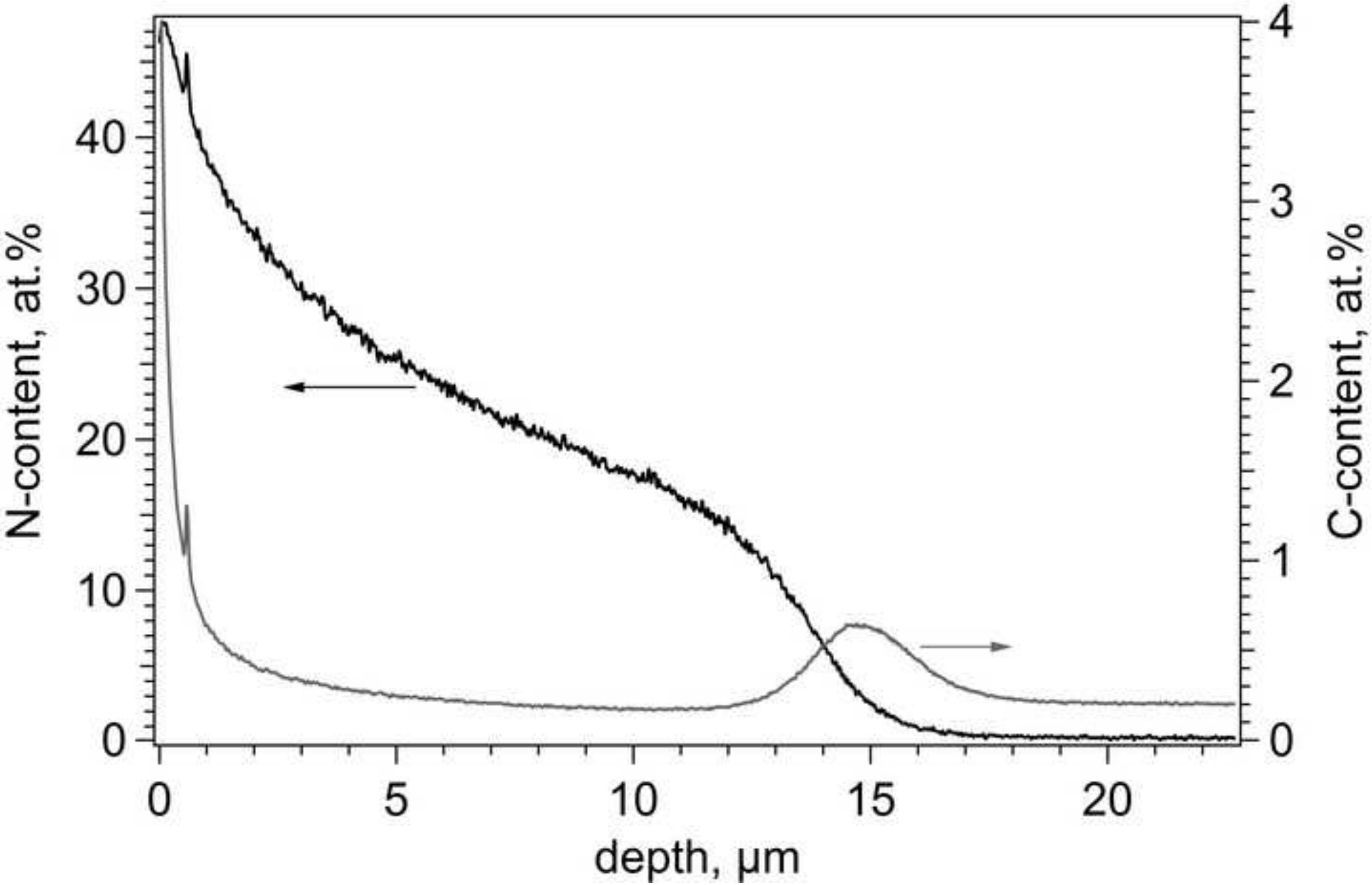

Figure 4

Click here to download high resolution image

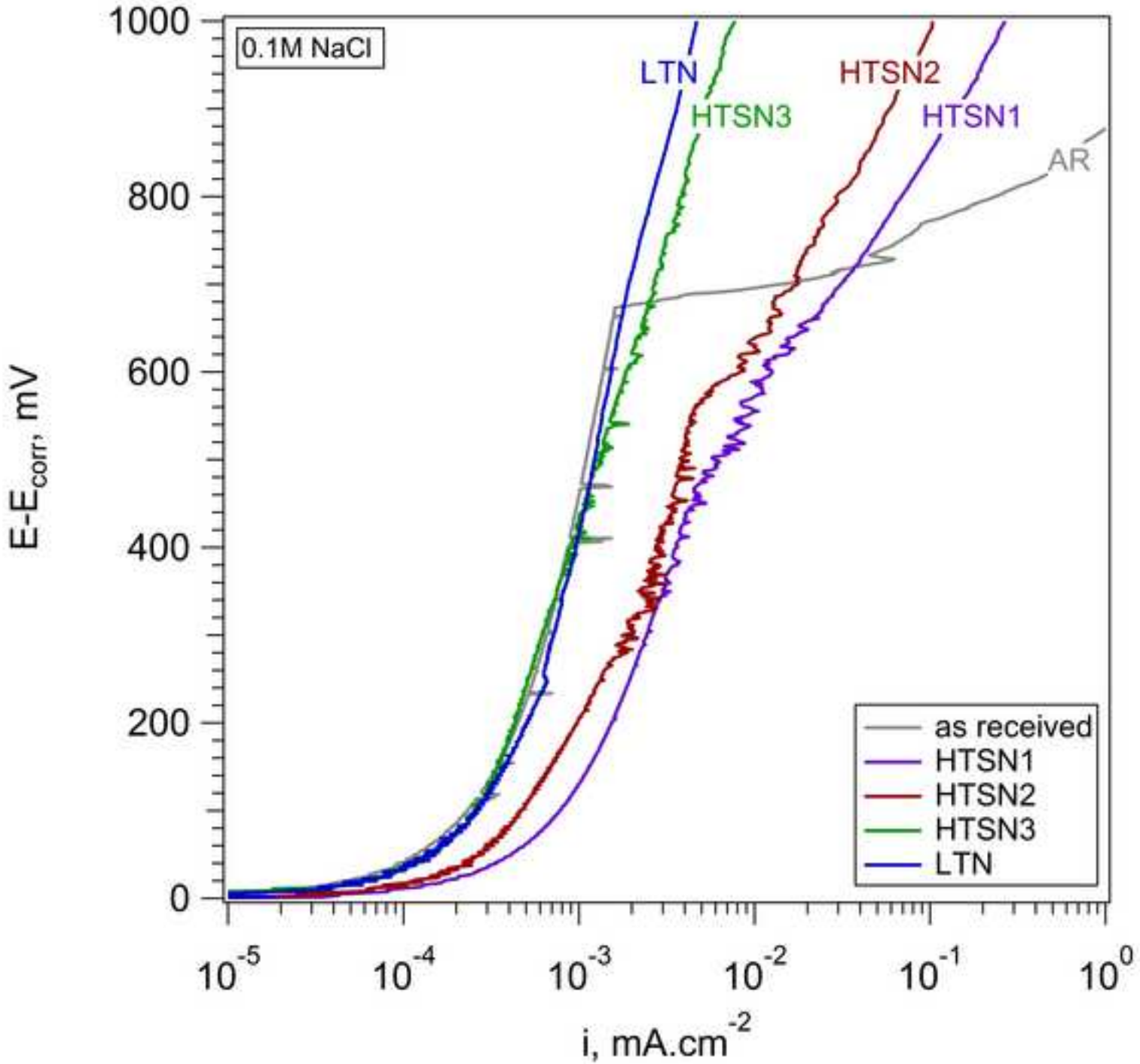

Figure 5

Click here to download high resolution image

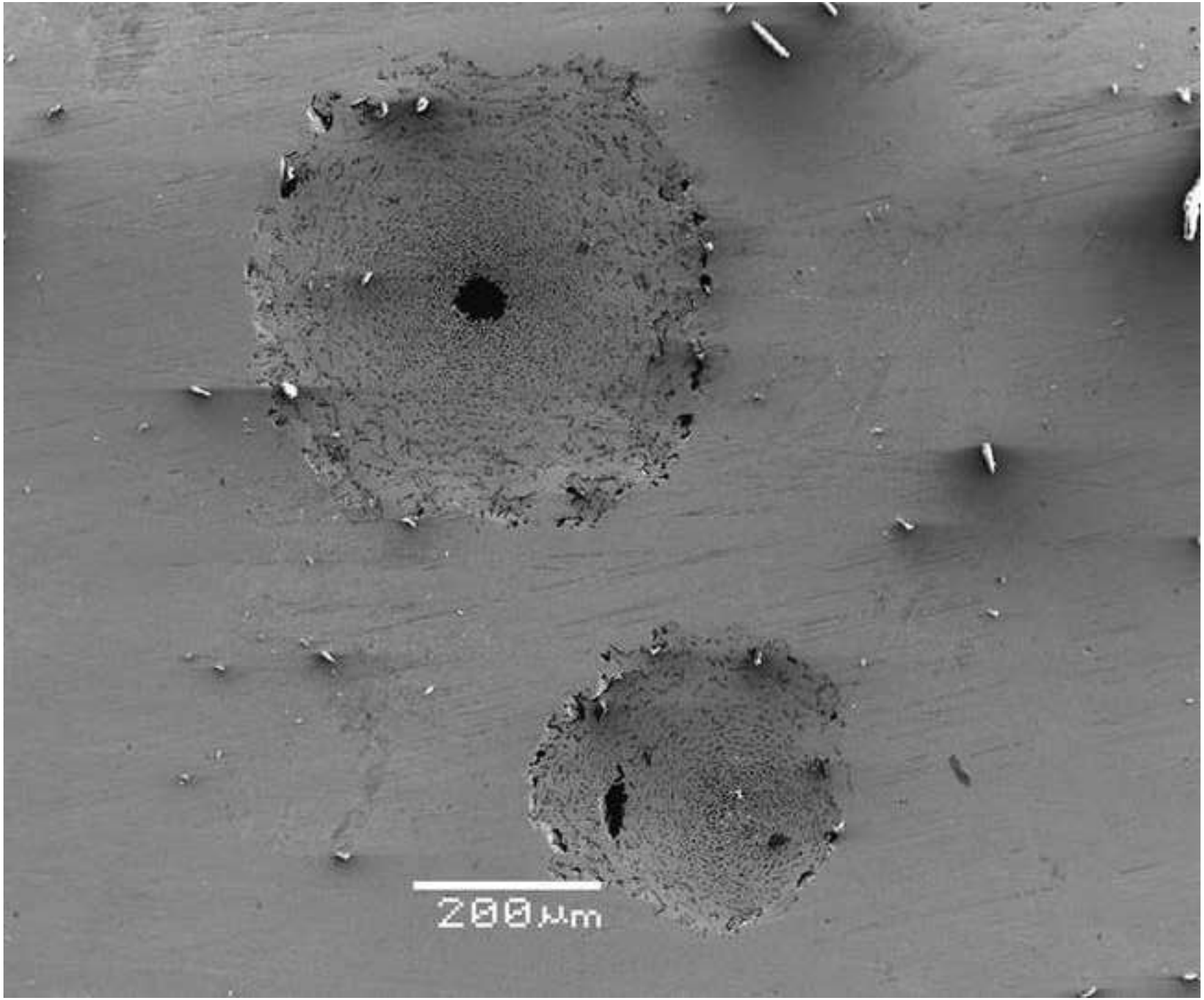

Figure 6a

Click here to download high resolution image

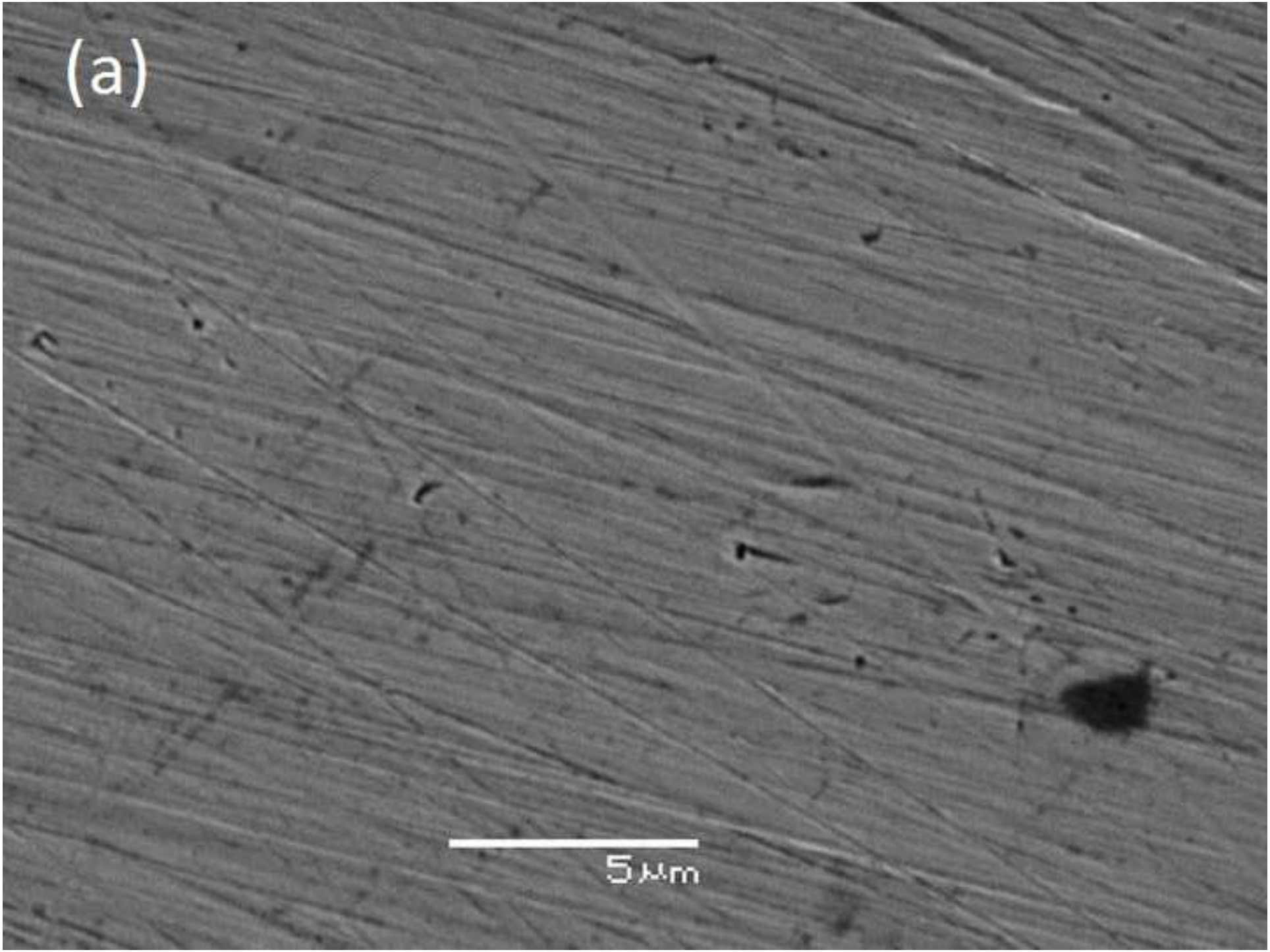

Figure 6b

Click here to download high resolution image

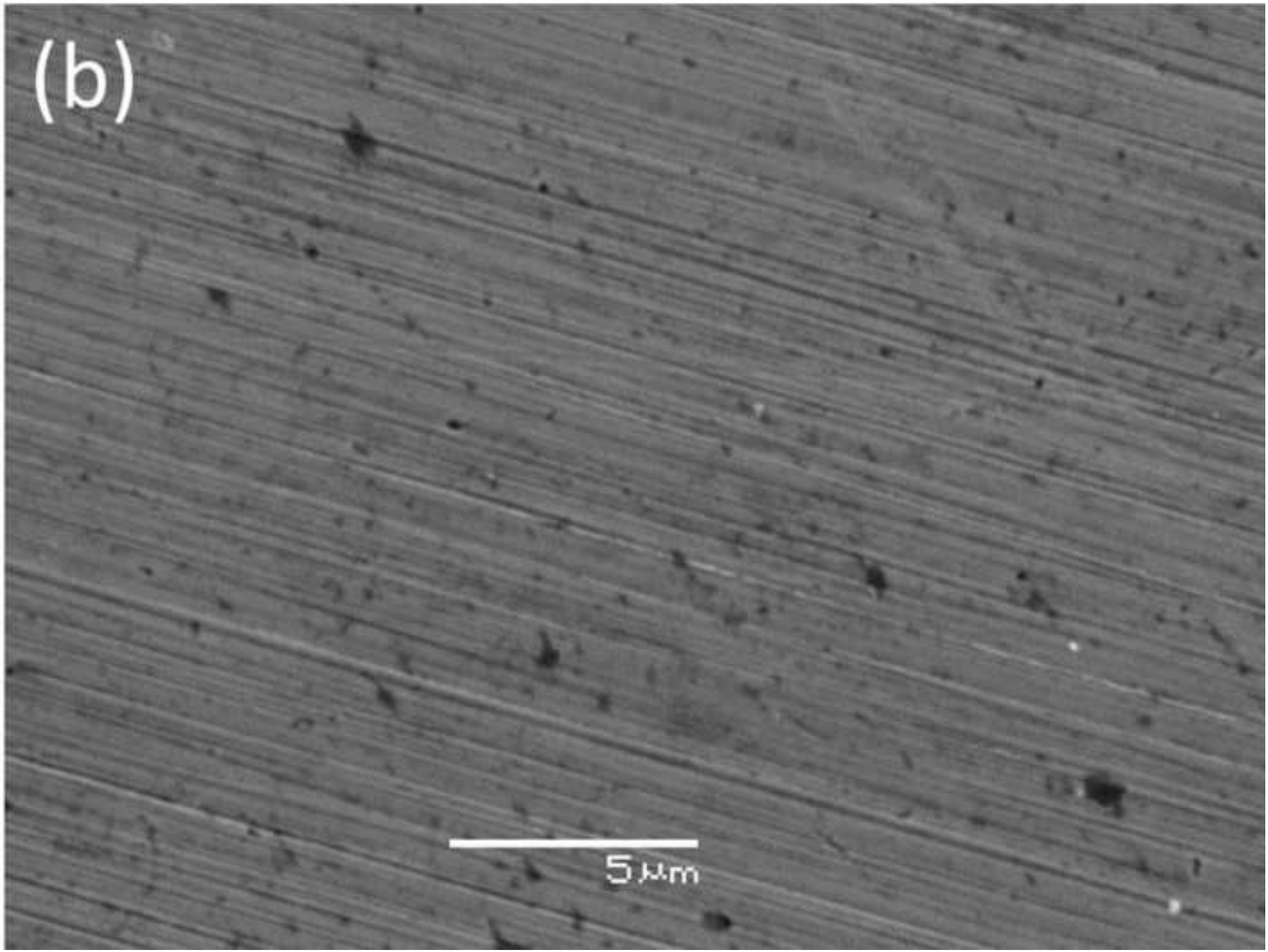

Figure 6c

Click here to download high resolution image

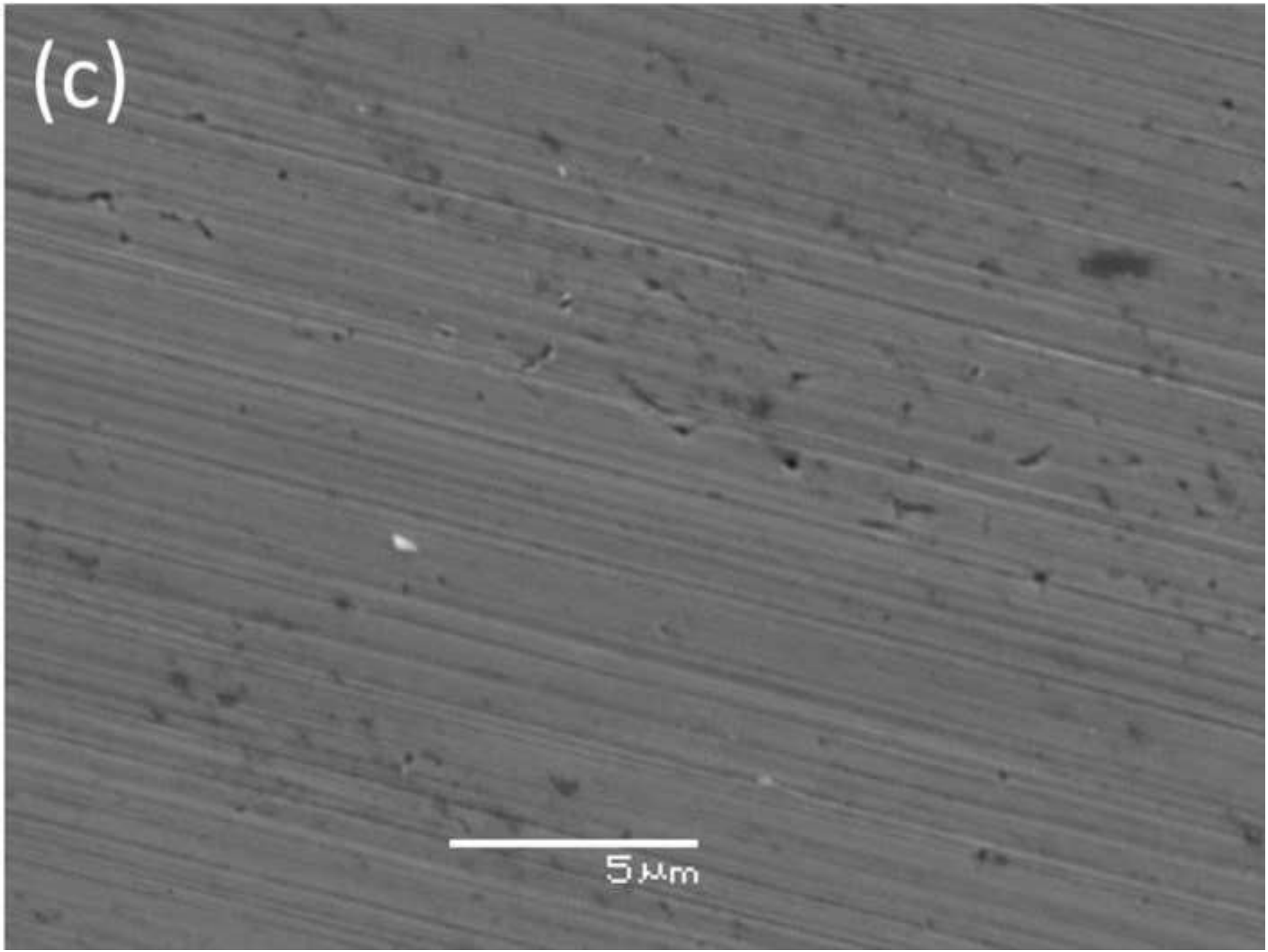

Figure 7

Click here to download high resolution image

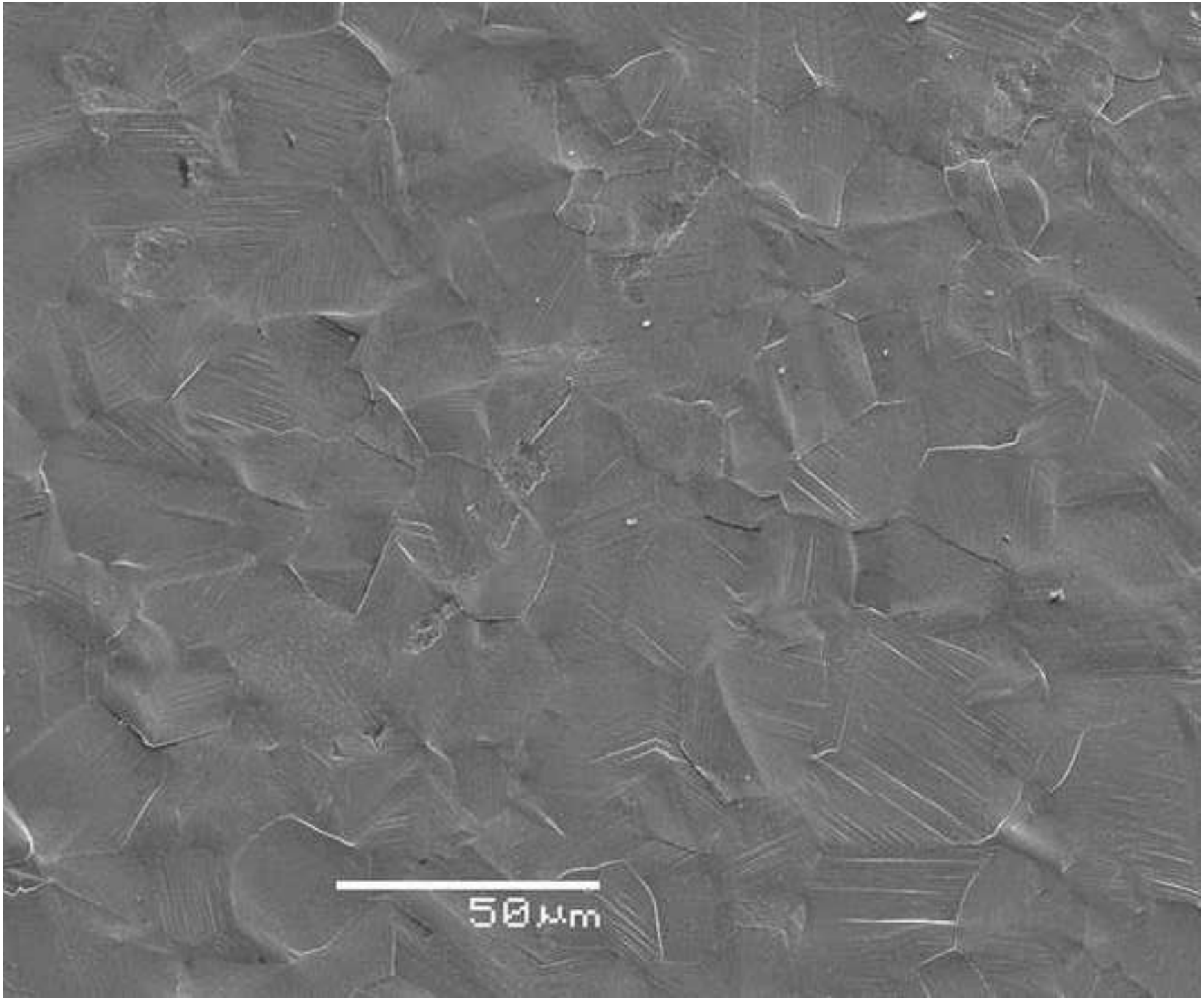

Figure 8

Click here to download high resolution image